Submicron Particles of SBA-15 Modified with MgO as Carriers for Controlled Drug Delivery

Shoucang SHEN,* Pui Shan CHOW, Fengxi CHEN, and Reginald Beng Hee TAN

Institute of Chemical and Engineering Sciences; 1 Pesek Road, Jurong Island, Singapore 627833, Republic of Singapore.
Received December 12, 2006; accepted April 19, 2007

Submicron particles with modified surface were synthesized by a simple one-pot synthesis approach and used as drug carrier for controlled release. Due to the alkalinity of MgO species on the surface, the amount of a model drug, ibuprofen, adsorbed on the modified surface was increased as compared to pure silica SBA-15 although the surface area was decreased by the surface modification. FTIR investigation indicated that the adsorption state of ibuprofen on MgO modified SBA-15 was different from that on pure silica SBA-15 and pure crystal ibuprofen. The result obtained from *in vitro* release test exhibited that the surface modification greatly decreased the ibuprofen release rate. In first 6 h *in vitro* release test, only 63% of the adsorbed ibuprofen was released from the MgO/SBA-15 (Si/Mg=20). In contrast, the release of ibuprofen was complete in 1 h from the pure silica SBA-15 under the same release conditions. The surface modified with MgO created affinity with acidic ibuprofen molecules and retarded the release rate from the mesoporous matrix. In addition, the release rate of ibuprofen could be modulated by varying the content of MgO, and was found to decrease with increasing amount of MgO on surface of SBA-15 submicron particles.

Key words submicron; SBA-15; MgO-modified; controlled release; ibuprofen; drug delivery

Controlled drug delivery technology represents one of the most rapidly advancing areas of biomedical science contributed by chemists and chemical engineers to health care. Controlled delivery systems offer significant advantages over conventional dosage forms, in terms of enhanced efficiency of medicine, and improved patient compliance and convenience over as the efficiency of medicine. The method by which a drug is delivered can have a significant effect on its therapeutic efficacy. The controlled drug release process is attractive and has been widely and intensively studied. Much of this work involves polymers to enable the drug to be delivered at relative constant rate by diffusion control from polymer or polymer composites over time.[1—7] The drug is deposited by means of direct compression, coating, wet granulation, or mechanical mixture of both matrix and drug. These methods have in general the disadvantage of non-uniform distribution, which can influence the release rate between different drug compositions. Therefore, much improvement in this field would be expected if chemically homogeneous materials possessing uniformly arranged porosity to accept organic guest molecules are made available.

Novel ordered mesoporous silica materials with biocompatible amorphous pore walls fulfill these requirements and have good potential for biomedical applications of drug delivery and tissue regeneration.[8—10] The large pore volume allows high drug loading into the ordered matrix. The large surface area of the internal surface can be modified according to specific purposes for different drugs association on the surface of matrix. Since Vallet-Regi and co-workers[11] reported that MCM-41 loaded ibuprofen could be sustained-release in 80 h, mesoporous silica materials have attracted great attention to be a potential controlled drug delivery system. Organic modified MCM-41 with functional groups on the surface could further decrease the delivery rate of ibuprofen.[12—15]

Among mesoporous materials, SBA-15 possesses a hexagonal array of mesopores 6.0—20 nm in diameter, which is much larger than the 3.0-nm pores characteristic of the MCM-41 and MCM-48. Therefore, SBA-15 mesoporous materials could be modified with various surface functional groups and still preserve the large pore channels and surface areas for drug adsorption and desorption.[16—19] It is expected to provide greater versatility for the delivery of drug molecules, whereupon the release rate depends to the large extent on the surface properties of drug carrier. The most common morphology of SBA-15 used is noodle-like fiber bundles of several tens of micrometers in length.[20] Particle size and morphology are among the significant factors to affect the uptake of formulated drugs through the intestine wall to body fluids for controlled delivery. Thus, it is important to develop mesoporous silica SBA-15 with submicron particle size and having new possibilities for incorporating biological agents within the silica host and for controlling their release kinetics from the matrix.[21] In this work, MgO-modified submicron mesoporous silica SBA-15 was prepared by one-pot hydrothermal synthesis route.[22] The functionalized surface of the submicron particles with moderate basic properties was used for the controlled release of drug substances using ibuprofen as a model drug with acidic groups.

Experimental

Synthesis of Materials MgO modified submicron SBA-15 particles were synthesized by one-pot hydrothermal treatment and *in-situ* coating process. Typically, 4.0 g of Pluronic P123 ($EO_{20}PO_{70}EO_{20}$, Aldrich) was dissolved in 150.0 g of 2 N HCl solution at 40 °C under vigorous stirring in 2 h. A certain amount of $Mg(NO_3)_3 \cdot 6H_2O$ (Sigma-Aldrich) was introduced to the solution under stirring to form a homogenous solution. Eight and one-half grams of tetraethyl orthosilicate (TEOS, Sigma-Aldrich) was added and stirred vigorously for 2 min. The mole ratio of components for the mixture is $SiO_2 : P123 : MgO : HCl : H_2O = 1.0 : 0.016 : x(0—0.2) : 6.9 : 178.6$ where x varies in range of 0—0.2 corresponding to different loading level of MgO. Then the mixture was kept under static conditions at 40 °C for 2 h, followed by a hydrothermal treatment at 100 °C for 24 h. The resulting material was directly evaporated at 100 °C for 24 h. The material was heated from room temperature to 550 °C at a heating rate of 2°/min and followed by calcinations in air for 6 h.

Drug Loading To load ibuprofen onto MgO modified SBA-15 materials, 0.8 g of powder silica SBA-15 was added to 20 ml of ibuprofen–hexane solution with initial concentration of 40 mg/ml and adsorption was conducted for 48 h under stirring at room temperature. The powder was filtered

* To whom correspondence should be addressed. e-mail: shen_shoucang@ices.a-star.edu.sg

and dried at 40 °C under air flow for 24 h. The amount adsorbed on the samples was measured by thermogravimetric analysis (TGA).

***In Vitro* Drug Release Studies** One-half of drug-loaded material was pressed into a tablet (13×5 mm) by a pressure of 7.5 MPa. The dissolution profile was measured using the standard a USP dissolution tester (VK7010, Varian Co, U.S.A.) operated at 37±0.1 °C and stirring rate of 50 rpm. Each 0.5 g tablet was introduced into in the vessel with 500 ml of simulated body fluid (SBF) and drug release kinetic studies were performed. Simulated body fluid (SBF) has a composition very similar to the human plasma (mixed solution of: 136.8 mM of NaCl, 4.2 mM of $NaHCO_3$, 3 mM of KCl, 1.0 mM of $K_2HPO_4 \cdot 3H_2O$, 1.5 mM of $MgCl_2 \cdot 6H_2O$, 2.5 mM of $CaCl_2 \cdot H_2O$ and 0.5 mM of Na_2SO_4). The solution was buffered at pH 7.4 with 50 mM of tri(hydroxymethyl)aminometahane). A sample of the release medium (3.0 ml) was extracted for analysis at regular time intervals using a syringe, and replaced with the same volume of fresh SBF. The drug concentration released into SBF with time was measured by UV–vis spectrophotometer (UV3010 SHIMDZU) at a wavelength of 272 nm. Calculation of the corrected concentration of replaced ibuprofen is based on the following equation: $C_{torr}=C_t+v(C_0+C_1\cdots+C_{t-1})/V$, where C_{torr} is the corrected concentration at time t, C_t is the apparent concentration at time t, v is the volume of sample taken and V is the total volume of the dissolution medium in vessel.[23]

Characterization All solid samples were characterized by X-Ray Diffraction (XRD), Scanning Electronic Microscopy (SEM), Fourier Transform Infra Red (FTIR) spectroscopy, The transmission electron microscopic (TEM), and N_2 adsorption. X-ray diffraction measurements were performed on a D8-ADVANCE (BRUKER, U.S.A.) X-ray diffractometer in steps of 0.02° using Cu$K\alpha$ radiation as X-ray source. The unit cell parameter (a_0) was calculated using the formula $a_0=2d_{100}/\sqrt{3}$, where d_{100} represented the d-spacing value of the (100) diffraction peak in XRD patterns of the samples. SEM images were taken with a field emission scanning electron microscope (FESEM, JEOL JSM-6700F, JEOL Co., Japan). The framework vibration FTIR spectra were recorded on TFS3000MX (BIO-RAD, Bio-rad Lab., U.S.A.) infrared spectrophotometer at a resolution of 2 cm^{-1}. The samples were thoroughly ground with KBr pellet before being pressed at 4 ton to form a thin wafer and storage in a desiccator with silica gel desiccant under vacuum for 24 h prior to measurement. TEM measurement was performed on TECNAI F20 (G^2) (FEI, Netherlands) electron microscope at 125 kV. Nitrogen adsorption/desorption isotherms were measured by using an Autosorb-6B gas adsorption analyzer (Quantachrome, U.S.A.) at the temperature of −196 °C. Before nitrogen adsorption–desorption measurements, each sample was heated at 300 °C under vacuum for 12 h. The specific surface areas of the samples were determined from the linear portion of the Brumauer–Emmett–Teller (BET) plots. The pore size (diameter D_{BET}) distribution was calculated from the adsorption branch of N_2 adsorption–desorption isotherms using the conventional Barrett–Joyner–Halenda (BJH) method.

Results and Discussion

Characterization of MgO Modified SBA-15 Submicron Particles Figure 1 shows the low and high angle XRD patterns of samples of pure silica SBA-15 and SBA-15 *in-situ* modified with MgO. All samples exhibited typical XRD patterns of SBA-15 mesoporous materials. An intensive diffraction peak observed at $2\theta=0.84$—$0.98°$ for all samples corresponds to the (100) diffraction peak, accompanying with two small peaks assigned to (110) and (200), is characteristics of ordered structure of 2D hexagonal space group (*p6mm*).[24,25] As compared with pure silica SBA-15, the (100) diffraction for the MgO modified SBA-15 was shifted to lower angle, resulting in an increase in the corresponding unit cell parameter a_0. The unit cell parameter a_0 was 104 Å for pure silica SBA-15 and it was 118 Å for MgO/SBA-15 (Si/Mg=20). When the content of MgO was increased to Si/Mg=5, the diffraction peak of (100) shifted to 0.84° with a unit cell parameter of 121 Å. The high angle XRD patterns indicate that the pore wall of all samples of pure silica SBA-15 and MgO/SBA-15 was in an amorphous state. In addition, for the *in-situ* modified SBA-15 with MgO (Si/Mg=20), the diffraction of MgO was not observed, indicating that that MgO was highly dispersed onto the large internal pore surface or embedded in the amorphous pore wall without formation of crystalline MgO. When MgO/SBA-15 with MgO content increased to Si/Mg=5, only a very small diffraction peak appeared at 43°. As compared with MgO mechanically mixed with pure silica SBA-15, the diffraction peak due to modified MgO was extremely low although both samples possessed same MgO content (Si/Mg=5). The results suggest that most of the MgO was coated onto internal surfaces with high dispersion in the amorphous state even with the content as high as Si/Mg=5.

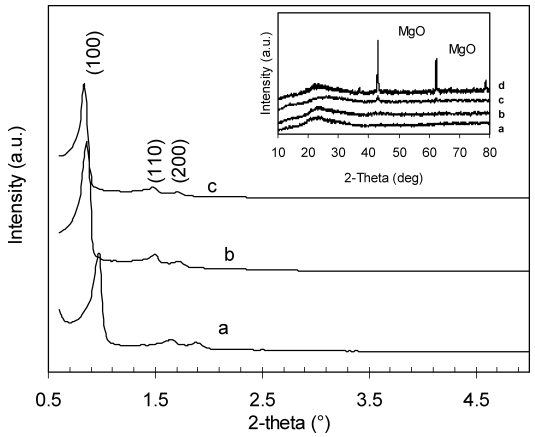

Fig. 1. Low Angle and High Angle (Inset) XRD Patterns of (a) Silica SBA-15 and (b) MgO/SBA-15 (Si/Mg=20), (c) MgO/SBA-15 (Si/Mg=5), (d) MgO Mixed with Pure Silica SBA-15 (Si/Mg=5)

Figure 2 displays FESEM images of submicron particles of pure silica SBA-15 and MgO modified SBA-15 with different Si/Mg ratios. Uniform submicron particles were observed for both samples synthesized by static hydrolysis of TEOS for 2 h and followed by a hydrothermal treatment of the gel mixture at 100 °C. The average particles size was slightly increased with the presence of Mg^{2+} in solution mixture during synthesis. For pure silica SBA-15, particle size was 0.5—0.8 μm and it was 0.7—0.9 μm for the two samples of MgO-modified SBA-15. Nevertheless, the particle size of resultant MgO modified SBA-15 was well-confined in submicron range and the particles were well dispersed. The surface morphology of submicron mesoporous silica particle was not affected by the presence of $Mg(NO_3)_3$ in synthesis media. Wei and co-workers[22,26] have reported that MgO could be *in-situ* coated on to SBA-15 mesoporous materials. By stirring continuously during hydrolysis of TEOS in the strong acidic P123 polymer solution, fiber-like MgO modified SBA-15 with particle size of 10—100 μm was obtained. The stirring condition during the self-assembly process was found to affect the morphology of SBA-15 materials significantly.[27] Rod-like particles with length of 1—2-μm formed under static hydrolysis and self assembly conditions.[21] The monodispersed submicron SBA-15 particles were found to be formed in first 2 h of static hydrolysis of TEOS and self-assembly of silica species on P123 polymer micelles.[28] The subsequent hydrothermal treatment consolidated the pore wall and helped to maintain the uniform mesoporous structure upon calcinations. Although it has been found that the morphology of SBA-15 materials were greatly influenced by

the inorganic salt in reaction mixtures[29,30] in this study, $Mg(NO_3)_3$ was not found to influence the surface morphology of resulting submicron SBA-15 particle. As the uptake of drug carrier was found to significantly depend on the particle size,[31] the highly dispersed submicron particle as drug carriers would facilitate the uptake of active pharmaceutical ingredient (API) through oral administration.

Figure 3 shows the transmission electron microscopy (TEM) images of MgO/SBA-15 (Si/Mg=5) submicron particles at different orientations. Figure 3A clearly indicates that the hexagonal pores with diameter of *ca.* 8 nm are perfectly stacked and Fig. 3B shows the parallel mesoporous channels formed in submicron particle.

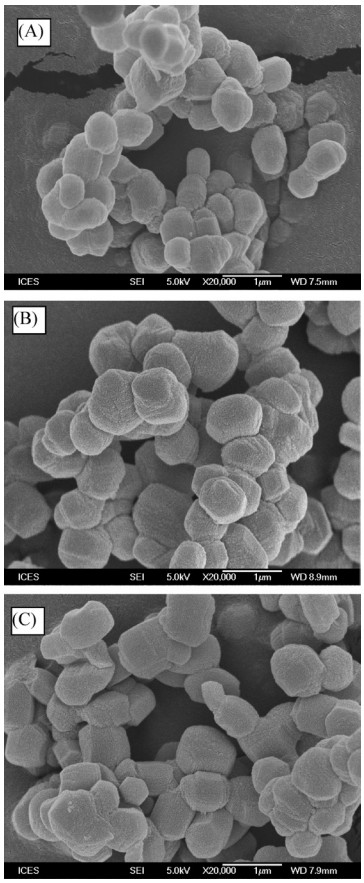

Fig. 2. FESEM Images of (A) Pure Silica SBA-15 and (B) MgO/SBA-15 (Si/Mg=20) and (c) MgO/SBA-15 (Si/Mg=5) Submicron Particles

Figure 4 shows the N_2 adsorption–desorption isotherms of pure silica SBA-15 and MgO/SBA-15 submicron particles. All samples exhibited typical type IV isotherms comprising H_1 type hysteresis with parallel adsorption and desorption branches, reflecting the regular array of cylindrical pore structure of SBA-15 materials.[32] The amount of N_2 adsorption slightly decreased for the MgO-modified submicron SBA-15 (Si/Mg=20) compared to the pure silica SBA-15. With the increase of MgO content, the amount of N_2 adsorption decreased. The surface areas were decreased by *in-situ* coating of MgO onto the surface of SBA-15 submicron particles. With Si/Mg=20, the surface areas was slight reduced from 725 to 693 m^2/g and total pore volume reduced from 1.03 to 1.02 cc/g as compared to pure silica SBA-15. When the MgO content increased to Si/Mg=5, the surface area and pore volume decreased to 596 m^2/g and 0.87 cc/g, respectively. However, the pore size was not decreased by *in-situ* coating MgO onto SBA-15 materials, because the pore size was determined by the size of surfactant micelles in the synthesis media. With the presence of $Mg(NO_3)_3$ during the self-assembly of silica-surfactant and followed by hydrothermal treatment and direct drying, the resulting pore wall was

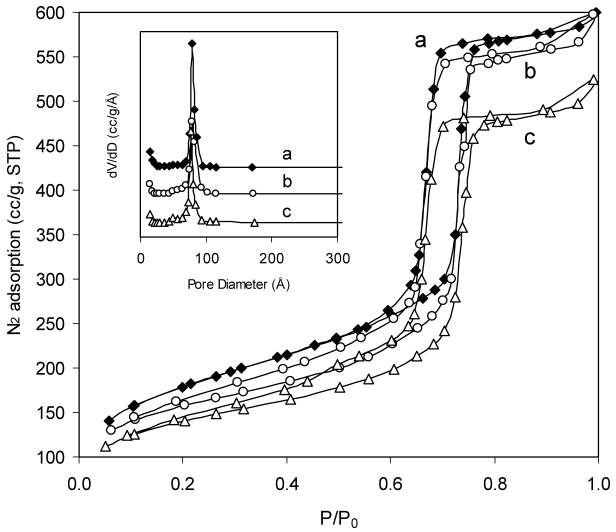

Fig. 4. N_2 Adsorption–Desorption Isotherms and Pore Size Distribution of Submicron Particles (a) Pure Silica SBA-15, (b) MgO/SBA-15 (Si/Mg=20), and (c) MgO/SBA-15 (Si/Mg=5)

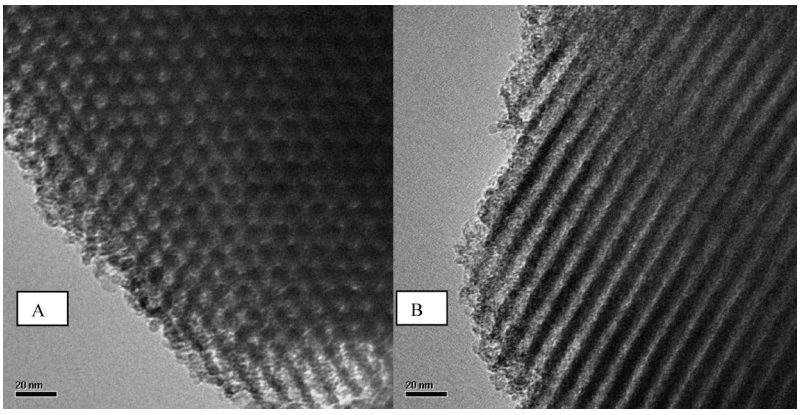

Fig. 3. TEM Images of MgO/SBA-15 (Si/Mg=5) Submicron Particles: (A) Taken along the Parallel Pore Channels and (B) Taken Vertical to the Parallel Pore Channels

Table 1. Pore and Surface Properties and Drug Loadings of SBA-15 Submicron Particles Modified with MgO

Sample	a_0 (nm)	D_{BET} (nm)	S_{BET} (m^2/g)	V_T (cc/g)	Ibuprofen loading (wt%)
SBA-15	10.4	7.9	725	1.03	15.8
MgO/SBA-15 (Si/Mg=20)	11.8	8.0	693	1.02	28.6
MgO/SBA-15 (Si/Mg=5)	12.1	8.0	569	0.87	32.2

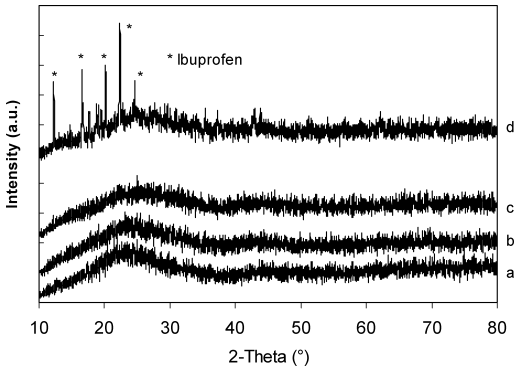

Fig. 5. XRD Patterns of Ibuprofen Loaded on Submicron Particles of (a) Pure Silica SBA-15, (b) MgO/SBA-15 (Si/Mg=20), (c) MgO/SBA-15 (Si/Mg=5) and (d) 30 wt% Ibuprofen Mixed with Pure Silica SBA-15

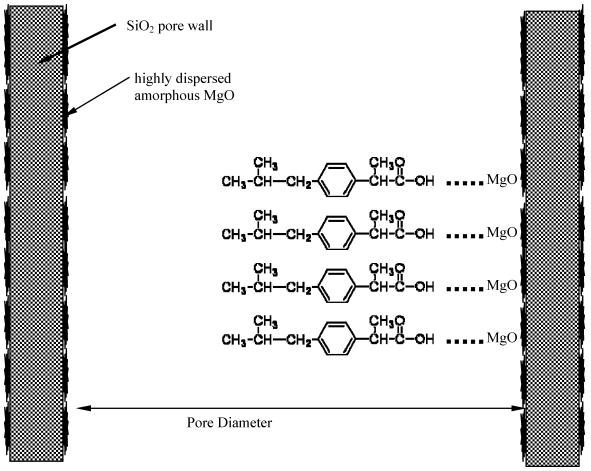

Fig. 6. Illustration of Ibuprofen Molecules Adsorption States on MgO/SBA-15 Material

thicker with larger cell parameter. After removal of the soft template surfactant by calcination, the pore size remained constant as the size of the surfactant micelle was not affected by Mg^{2+} in the solution. Thus the thicker pore wall caused by MgO-coating led to the decrease of surface area and total pore volume of the resultant mesoporous materials.

Drug Loading on MgO-SBA-15 Submicron Particles The drug loading of ibuprofen on SBA-15 and MgO-modified SBA-15 materials is tabulated in Table 1. It is found that drug loading is increased on MgO-modified SBA-15 materials, although the MgO modified SBA-15 submicron particles have smaller surface area and pore volume. As indicated in Table 1, the loading of ibuprofen on pure silica SBA-15 was only 15.8 wt%; as a comparison, MgO/SBA-15 (Si/Mg=20) submicron particles adsorbed 28.6 wt% of ibuprofen although its surface area was lower than pure silica SBA-15. With increase of MgO content to Si/Mg=5, the ibuprofen loading was increased to 32.2% due to more adsorption sites created. MgO is a basic material that is widely used as an alkaline adsorbent and as a catalyst.[33—36] MgO modified SBA-15 has been proven to create basic sites on the large surface of SBA-15 materials and significantly improves its adsorption with acidic gases on mesoporous materials.[22,26] When ibuprofen was loaded on to mesoporous submicron particles through adsorption from hexane solution, the MgO modified SBA-15 has higher affinity with acidic drug molecules, thus resulting in higher drug loading.

The adsorbed ibuprofen on SBA-15 materials was found to be in the amorphous state. As shown in Fig. 5, ibuprofen loaded on all SBA-15 submicron particles lacked X-ray diffraction peaks, indicating that no crystallization occurred inside the nanopore channels. Due to the large surface area of SBA-15, ibuprofen was highly dispersed or adsorbed on the surface of SBA-15 when the drug was loaded by adsorption from solution. According to a previous investigation of crystallization processes in confined spaces, crystallization can only occur in channels with diameter to molecular size ratios above 20.[37] The pore diameter in this study was about 8 nm in this study, which is about 8 to 13 times of the dimension of the ibuprofen molecule (estimated to be 1.0×0.6 nm).[11] As a comparison in Fig. 5, 30 wt% of ibuprofen mixed with SBA-15 clearly exhibited the diffraction peaks characteristic for crystals of ibuprofen. The adsorption state of ibuprofen on MgO/SBA-15 is illustrated in Fig. 6. Ibuprofen molecules were adsorbed on the highly dispersed MgO on internal surface of modified SBA-15 particles. The affinity of acidic molecules and modifier is believed to retard the drug release from modified drug carrier. For pure silica SBA-15, ibuprofen molecules were weakly and directly attached with surface of silica pore wall.

Figure 7 shows that the FESEM images of ibuprofen loaded SBA-15 and MgO/SBA-15 (Si/Mg=5). The morphology of the submicron particles of SBA-15 was well preserved after drug loading. As the large surface area of SBA-15 mesoporous material is mostly contributed by internal surface area, most of drug molecules adsorbed on the surface of pore channel inside the submicron particles. The outer surface morphology of the resultant ibuprofen loaded SBA-15 was not changed by drug adsorption even though the drug loading was up to 30 wt%.

Drug Release Figure 8 exhibits the percentage of ibuprofen released as a function of time for ibuprofen loaded on pure silica SBA-15 and MgO-modified SBA-15 submicron particles. It was observed that the release was very fast for ibuprofen loaded on pure silica SBA-15 materials, reaching 100% release in 1 h. This dissolution rate was found to be even faster than that of bulk pure ibuprofen crystal in tablet form, where it needed 5 h to reach 95% of dissolution under same dissolution condition. It was also reported that more

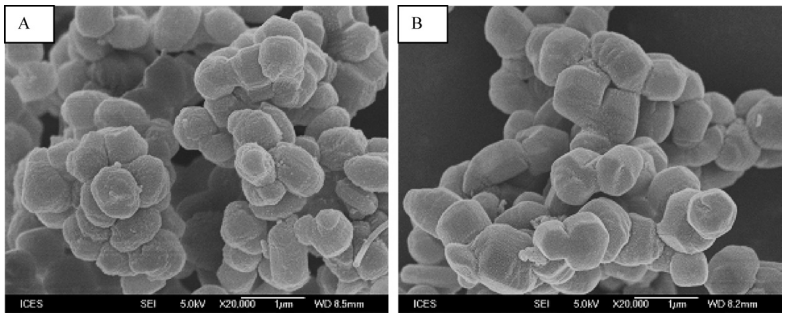

Fig. 7. FESEM Images of Ibuprofen Loaded Submicron Particles of (A) Pure Silica SBA-15 and (B) MgO/SBA-15 (Si/Mg=5)

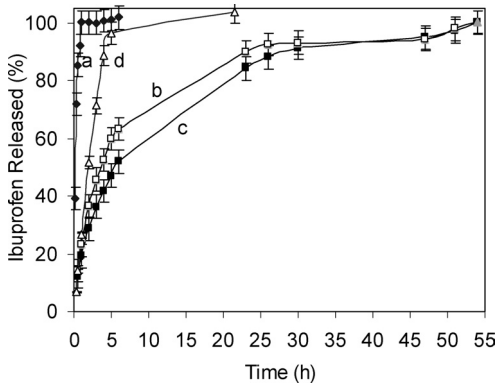

Fig. 8. Cumulative Release Profiles for Ibuprofen Loaded on Submicron Particles of (a) Pure Silica SBA-15, (b) MgO/SBA-15 (Si/Mg=20), (c) MgO/SBA-15 (Si/Mg=5); and (d) Pure Ibuprofen Tablet

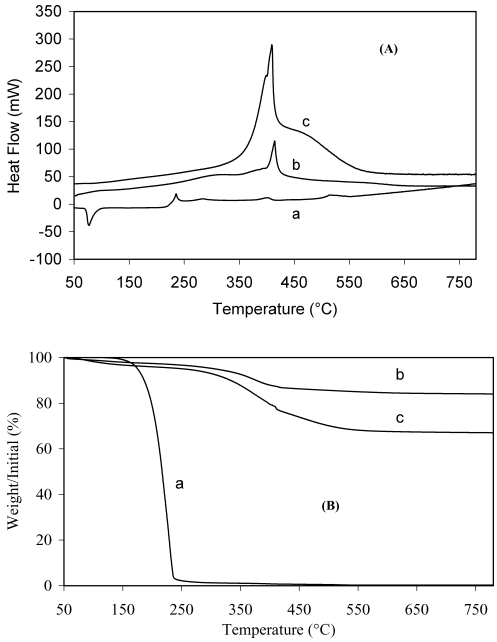

Fig. 9. DSC (A) and TGA (B) Profiles of (a) Pure Ibuprofen Crystal, (b) Ibuprofen Loaded on Pure Silica SBA-15 and (c) Ibuprofen Loaded on MgO/SBA-15 (Si/Mg=5) Submicron Particles

than 2 h was needed for complete dissolution.[38] The dissolution of amorphous ibuprofen loaded on pure silica SBA-15 is facilitated as compared with pure ibuprofen crystal. This result is greatly different from that of ibuprofen loaded on pure silica MCM-41,[11] where it showed a slow controlled release rate although both carriers have large surface areas. The discrepancy could be due to difference in pore size and morphology of drug carriers. In this study, the pore size of SBA-15 (*ca.* 8 nm) was much larger than that of MCM-41 (2—3 nm). In addition, the length of the submicron SBA-15 particles used in this study was much shorter than the MCM-41 used in the comparable case. As ibuprofen was finely dispersed on pure silica SBA-15 in the amorphous state and the interaction with the substrate was weak, the large pore size and short pore channel resulted in a faster dissolution rate than pure ibuprofen crystal pellets. However, ibuprofen adsorbed on MgO-modified SBA-15 submicron particles exhibited a much slower release rate. It required more than 50 h to reach 100% release of ibuprofen adsorbed. In the first 6 h, 63% of adsorbed ibuprofen was released from MgO/SBA-15 (Si/Mg=20). With increase of MgO content, the release rate was further delayed. Only 52% of ibuprofen was released from MgO/SBA-15 (Si/Mg=5) in the first 6 h. After 6 h, the release rate of ibuprofen decreased noticeably, with a further decrease in rate at around 25 h. The delayed release of ibuprofen from MgO-modified SBA-15 is believed to be attributed to the interaction between ibuprofen molecules and alkaline functional surface. This suggests that the release rate of ibuprofen can be tuned by varying the content of MgO in MgO-modified SBA-15 submicron particles.

DSC Study on Ibuprofen Loaded Samples Figure 9 depicts the DSC-TGA profiles of ibuprofen loaded on different carriers and as comparison with pure crystal ibuprofen. For pure ibuprofen, an endothermic peak at 78 °C corresponding to the melting point of crystal ibuprofen was observed. This kind of endothermic peak due to melting of bulk ibuprofen was not detected for ibuprofen adsorbed on the SBA-15 submicron particles as ibuprofen molecules were adsorbed on the large surface in a highly dispersed state. In the temperature range of 300—550 °C, a strong exothermic peak was found for ibuprofen loaded on MgO/SBA-15 (Si/Mg=5) mesoporous material, due to the oxidation of ibuprofen molecules in air. This strong exothermic peak corresponded to the weight loss of ibuprofen in TGA curves (Fig. 9B). As the drug loading on pure silica SBA-15 submicron particle was much lower, the exothermic peak caused by the oxidation of adsorbed ibuprofen was smaller than that on MgO modified SBA-15. For pure ibuprofen, only a small exothermic peak was observed at the temperature region of 220—250 °C and the strong exothermic peak at temperature of 300—550 °C was not appeared. In the Fig. 9B, a quick weight loss at 150—250 °C for pure ibuprofen was observed, due to the

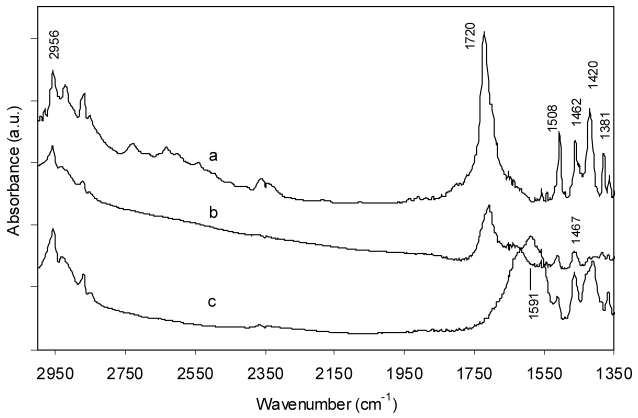

Fig. 10. FTIR Spectra of (a) Pure Ibuprofen Crystal, (b) Ibuprofen Loaded on Pure Silica SBA-15 and (c) Ibuprofen Loaded on MgO/SBA-15 (Si/Mg=5)

evaporation of ibuprofen. As the melted pure ibuprofen vaporized below the temperature for oxidation reaction, thus exothermic effect was not as strong as that of ibuprofen adsorbed on SBA-15 materials at 300—550 °C. Ibuprofen strongly adsorbed on MgO/SBA-15 did not evaporate above the boiling point of ibuprofen, and it was oxidized on carriers in the air at the higher temperature range depending on the affinity of molecules and adsorption sites on the surface.

FTIR Investigation on the Interaction of Drug and Carriers FTIR investigation provides the evidence of the interaction of ibuprofen molecule with MgO-modified surface. As shown in Fig. 10, the sample of pure ibuprofen exhibits a strong band at 1720 cm^{-1}, attributed to the ν(C=O) stretching vibration for free ibuprofen molecules.[39] The weak bands at 1508 and 1462 cm^{-1} could be assigned to ring vibrations of the organic molecules.[40] Typical ν(CH) stretching vibrations of ibuprofen are observed at 2958, 2927, and 2871 cm^{-1} for pure ibuprofen as well as that loaded on different support.[40] For ibuprofen loaded on pure silica SBA-15 submicron particles, the band around 1720 cm^{-1} still existed. However, for ibuprofen loaded on MgO-modified SBA-15, this characteristic band for carboxyl C=O stretching vibration of free ibuprofen was not observed. A new broad band at 1591 cm^{-1} was detected, which could be due to the partially transfer of proton from the carboxylic acid of ibuprofen to the basic sites of modified surface. It has been reported that, when ibuprofen adsorbed on amino-functional silica mesoporous materials, the band corresponding to ν(C=O) stretching shifted from carboxylic values to the carboxylate value.[41,42] An absorbance band at 1558 cm^{-1} was found for ibuprofen adsorbed on amino-group grafted SBA-15, and it was assigned to the asymmetric stretching vibration of COO^-.[43] In this study, the alkalinity of MgO modified SBA-15 was not as strong as amino groups, the donation of proton from COOH was not fully accepted as that of amino-functioned surface. Thus, the IR band of C=O stretching shifts to 1591 cm^{-1} for ibuprofen adsorbed on MgO-modified SBA-15 submicron particles. These results imply that the alkalinity of pore wall surface play a significant role for adsorption and delivery of acidic drug molecules. The MgO-modified SBA-15 submicron particles apparently have stronger interaction with acidic drug molecules than pure silica SBA-15. FTIR results also indicated the interaction of ibuprofen and pure silica SBA-15 was very weak, thus the release rate of amorphous ibuprofen from pure silica SBA-15 was very fast. The chemical affinity of carboxylic group of ibuprofen with surface basic sites of Mg/SBA-15 resulted in the controlled release profiles. This application could be expanded to other acidic drug molecules with carboxylic groups.

Conclusion

The drug carriers of MgO-modified SBA-15 submicron particles synthesized by one-pot *in-situ* coating route demonstrated a simple, effective approach for well-controlled release of acidic drug molecules. Due to the alkaline MgO functional surface, the amount of ibuprofen adsorbed on MgO-modified SBA-15 was higher than pure silica SBA-15 although the surface area was decreased by MgO-coating. XRD results indicated that ibuprofen adsorbed on surface of SBA-15 was amorphous. The morphology of SBA-15 submicron particles was well preserved with drug loading up to 30 wt%. The results obtained from *in-vitro* test exhibited the surface coating of MgO greatly delayed the ibuprofen release rate, and the release rate was further decreased with increasing the amount of MgO coated onto the internal surface of SBA-15 submicron particles. Sustained release for time period up to 55 h could be reached from MgO-modified SBA-15, whereas 100% ibuprofen could be completed in less than 1 h from pure silica SBA-15 submicron particle under the same release condition. The delayed release profile from MgO-modified SBA-15 was attributed to the interaction of ibuprofen molecules with drug carrier surface, which was investigated by DSC-TGA and FTIR. TGA-DSC results indicated that adsorbed ibuprofen on SBA-15 desorbed greatly different from the pure ibuprofen crystal. A new FTIR band was observed on ibuprofen adsorbed on MgO-modified SBA-15 due to the proton transfer of ibuprofen to the alkaline functional surface, and the interaction was believed to be contributing factor in the controlled release of ibuprofen from carrier.

References

1) Davis K. A., Anseth K. S., *Critical Rew. Therapeutic Drug Carrier Systems*, **19**, 385—423 (2002).
2) Sinha V. R., Bansal K., Kaushik R., Trehan A., *Int. J. Pharm.*, **278**, 1—23 (2004).
3) McHugh A. J., *J. Control. Release*, **9**, 211—221 (2005).
4) Sendil D., Guresel I., Wise D. L., Hasirci V., *J. Control Release*, **59**, 207—217 (1999).
5) Yagmurlu M. F., Korkusuz F., Gursel I., Korkusuz P., Ors U., Hasirci V., *J. Biomed. Mater. Res.*, **46**, 494—503 (1999).
6) Wallace D. G., Rosenblatt J., *Adv. Drug Deliv. Rev.*, **55**, 1631—1649 (2003).
7) Qiu L. Y., Bae Y. H., *Pharm. Res.*, **23**, 1—30 (2006).
8) Vallet-Regi M. A., Ruiz-Gonzalez L., Izquierdo-Barba I., González-Calbet J. M., *J. Mater. Chem.*, **16**, 26—31 (2006).
9) Izquierdo-Barba I., Ruiz-González L., Doadrio J. C., González-Calbet J. M., Vallet-Regí M., *Solid State Sci.*, **7**, 983—989 (2005).
10) Tozuka Y., Wongmekiat A., Kimura K., Moribe K., Yamamura S., Yamamoto K., *Chem. Pharm. Bull.*, **53**, 974—977 (2005).
11) Vallet-Regi M., Ramila A., del Real R. P., Pariente J. P., *Chem. Mater.*, **13**, 308—311 (2001).
12) Munoz B., Ramila A., Pariente J. P., Diaz I., Vallet-Regi M., *Chem. Mater.*, **15**, 500—503 (2003).
13) Qu F. Y., Zhu G. S., Huang S. Y., Li S. G., Qiu S. L., *Chem. Phys. Chem.*, **7**, 400—406 (2006).
14) Tang Q. L., Xu Y., Wu D., Sun Y. H., Wang J. Q., Xu J., Deng F., *J. Control. Release*, **114**, 41—46 (2006).
15) Zeng W., Qian X. F., Zhang Y. B., Yin J., Zhu Z. K., *Mater. Res. Bull.*,

40, 766—772 (2005).
16) Doadrio J. C., Sousa E. M. B., Izquierdo-Barba I., Doadrio A. L., Perez-Pariente J., Vallet-Regi M., *J. Mater. Chem.*, **16**, 462—466 (2006).
17) Xia W., Chang J., *J. Control. Release*, **110**, 522—530 (2006).
18) Doadrio A. L., Sousa E. M. B., Doadrio J. C., Pariente J. P., Izquierdo-Barba I., Vallet-Reg M., *J. Control. Release*, **97**, 125—132 (2004).
19) Yang Q., Wang S. H., Fan P. W., Wang L. F., Di Y., Lin K. F., Xiao F. S., *Chem. Mater.*, **17**, 5999—6003 (2005).
20) Schmidt-Winkel P., Yang P., Margolese D. I., Chmelka B. F., Stucky G. D., *Adv. Mater.*, **11**, 303—307 (1999).
21) Sayari A., Han B. H., Yang Y., *J. Am. Chem. Soc.*, **126**, 14348—14349 (2004).
22) Wei Y. L., Wang Y. M., Zhu J. H., Wu Z. Y., *Adv. Mater.*, **15**, 1943—1945 (2003).
23) Fisher K. A., Huddersman K. D., Taylor M. J., *Chem. Eur. J.*, **9**, 5873—5878 (2003).
24) Zhao D. Y., Feng J., Huo Q., Melosh N., Fredrickson G. H., Chmelka B. F., Stucky G. D., *Science*, **279**, 548—552 (1998).
25) Zhao D. Y., Huo Q., Feng J., Chmelka B. F., Stucky G. D., *J. Am. Chem. Soc.*, **120**, 6024—6036 (1998).
26) Wang Y. M., Wu Z. Y., Wei Y. L., Zhu J. H., *Micropor. Mesopor. Mater.*, **84**, 127—136 (2005).
27) Kosuge K., Sato T., Kikukawu N., Takemori M., *Chem. Mater.*, **16**, 899—905 (2004).
28) Shen S. C., Chen F. X., Chow P. S., Phanapavudhikul P., Zhu K. W., Tan R. B. H., *Micropor. Mesopor. Mater.*, **92**, 300—308 (2006).
29) Schmidt-Winkel P., Yang P., Margolese D. I., Chmelka B. F., Stucky G. D., *Adv. Mater.*, **11**, 303—307 (1999).
30) Yu C., Fan J., Tian B., Zhao D. Y., Stucky G. D., *Adv. Mater.*, **14**, 1742—1745 (2002).
31) Jani P., Halbert G. W., Langridge J., Florence A. T., *J. Pharm. Pharmacol.*, **42**, 821—826 (1990).
32) Neimark A. V., Ravikovitch P. I., Vishnyakov A., *Phys. Rev. E*, **62**, R1493—1496 (2000).
33) Thomason P., Tyagi O. S., Knözinger H., *Appl. Catal. A*, **181**, 181—188 (1999).
34) Lavalley J. C., *Catalysis Today* **27**, 377—401 (1996).
35) Di Cosimo J. I., Díez V. K., Xu M., Iglesia E., Apesteguía C. R., *J. Catal.*, **178**, 499—510 (1998).
36) Liu Z., Cortés-concepción J. A., Mustian M., Amiridis M. D., *Appl. Catal. A*, **302**, 232—236 (2006).
37) Sliwinska-Bartkowiak M., Dudziak G., Gras R., Sikorski R., Radhakrishnan R., Gubbins K. E., *Colloid Surf. A: Physicochem. Eng. Aspects*, **187–188**, 523—529 (2001).
38) Costa F. O., Pais A. A. C. C., Sousa J. J. S., *Int. J. Pharm.*, **270**, 9—19 (2004).
39) Gordijo C. R., Barbosa C. A. S., Ferreira A. M. D. C., Constantino A. V. R. L., Silva D. D. O., *J. Pharm. Sci.*, **94**, 1135—1148 (2005).
40) Andrade A., Namora S. F., Woisky R. G., Wiezel G., Najjar R., Sertié J. A. A., Silva D. D. O., *J. Inorg. Biochem.*, **81**, 23—27 (2000).
41) Rámila A., Muñoz B., Pérez-Pariente J., Vallet-Regí M., *J. Sol-Gel Sci. Tech.*, **26**, 1199—1202 (2003).
42) Socrates G., "Infrared Characteristic Group Frequencies, Tables and Chatrs," Wily, New York, 1994.
43) Song S. W., Hidajat K., Kawi S., *Langmuir*, **21**, 9568—9575 (2005).